NUMERICAL STUDY OF SEPARATION FLOWS WITH LES/RANS HYBRID APPOACHES

Zhixiang XIAO, Haixin CHEN, and Song FU
Department of Engineering Mechanics, Tsinghua University, Beijing 100084, China
xiaotigerzhx@tsinghua.edu.cn, chenhaixin@tsinghua.edu.cn, fs-dem@tsinghua.edu.cn

ABSTACT

Large-eddy-simulation (LES) and Reynolds-Averaged Navier-Stokes (RANS) hybrid methods were applied for the separated flows at high angles of attack (AOA) around Aerospatial A-profile and prolate spheroid. These hybrid methods are based on algebraic Baldwin-Lomax (B-L) model through combining the similar profile of eddy viscosity of B-L and Smagrinsky sub-grid models, on Spalart-Allmaras (S-A) and Menter's k-ω shear-stress-transport (SST) models by replacing the length scale in the original turbulence models, and on Menter's k-ω SST model through a blending function The main objective of this paper is to apply the hybrid methods and compare with RANS methods based on the same turbulence models for high Reynolds separated flows. All the hybrid methods were designed to have a RANS mode near the solid wall and have a LES behavior in the core flow region. At the same time, fourth-order central scheme with particle artificial viscosity was applied as the spatial method and fully implicit Lower-Upper Symmetric-Gauss-Seidel with pseudo time sub-iteration (LU-SGS-τTS) was chosen as the temporal methods in this study. Comparison with experimental data was carried out for pressure, skin friction and the profiles of velocity, etc. Reasonable agreement, accounting the effect of turbulence models, was obtained for these separated flows.

INTRODUCTION

Three-dimensional (3-D) flow separation has been an interesting and challenging problem in fluid mechanics. Undesired effects such as loss of lift, increase in drag and amplification of unsteady fluctuations in the pressure fields always accompany when the 3-D separation takes place. 2-D separation flows are mainly dominated by the adverse pressure gradient, flow reversal, etc. In 3-D separation flows, the separation features can be sensitive to the body configuration, angle of attack and Reynolds number, etc.

In addition to the complex topology of the flow patterns, the 3-D separation flows strongly challenge analysis and predictive models. Analytical tools are much needed to provide accurate predictions of these flows to allow engineers to explore the underlying flow physics for better aero-propulsion flow components design and applications in the aerospace industry. The present work is focused on the numerical simulation for the 3-D separation flows around an Aerospatial A-profile and a 6:1 prolate spheroid. Recent calculations around Aerospatial A-profile include LES of Mellen et al. (2003), Davidson et al. (2000) and Morgan et al. (2003). The calculations around 6:1 prolate spheroid include the RANS calculation of Tsi et al. (1999), detached eddy simulation (DES) based on S-A model (Spalart and Allmaras, 1992) of Constantinescu et al. (2002) and LES of Wikström et al. (2004).

Current engineering approaches to the computation of turbulent flows are mainly based on the solution of RANS methods. Adequate accuracy and efficiency in steady flows without separation or flows recirculation can be obtained with them. It is, however, difficult to find an individual RANS turbulence model that can be used reliably to accurately predict dominating flows with massive separations.

The relatively poor performance for separation of RANS models has motivated the increasing application of Large Eddy Simulation. LES is known to resolve more turbulence details than the RANS model with modeling only small sub-grid scales of motion. LES has also been shown to provide accurate turbulent flow simulation at a fraction of cost of the direct numerical simulation (DNS). It is thus a powerful tool, providing a description of large, energy-containing scales of motion that are typically dependent on geometry and boundary conditions. When applied to boundary layers, however, the computational cost of whole-domain LES does not differ significantly from that of DNS. The "large eddies" close to the solid wall are physically small in scale. LES requires additional empiricism in treatment of the wall layer when LES is applied in the high Reynolds number flows.

To overcome the deficiencies of RANS models for predicting separation flows, an alternative modeling strategy of turbulence flows, often called as the hybrid methods of LES and RANS, has been proposed recently for predicting the unsteady and time-dependent separated flows. Such hybrid methods combine a standard turbulence model used in the region where turbulence is dominated by small scale with an LES-type treatment for the large scale motion in the core flow region.

So many kinds of LES/RANS hybrid methods have been developed in the last ten years. The initial hybrid method named as DES, which replaces the distance d from the nearest wall in S-A model with $\tilde{d} = \min(d, C_{DES}\Delta)$, was developed by Spalart et al (1997). Later, Speziale (1998) defines the stress tensor as $\tau_{ij} = [1-\exp(-\beta\Delta/L_k)]^n \tau_{ij}^{(R)}$, where L_k is Kolmogorov's length scale, Δ is representative grid size (or filter width), $\tau_{ij}^{(R)}$ is the Reynolds stress provided by a RANS model, and β and n are model constants. Strelets (2001) developed a DES-type hybrid method based on Menter's k-ω SST model (Menter, 1994) through introducing a length scale l in the turbulence kinetic transport equation and replacing it with the $\tilde{l} = \min(l, C_{DES}\Delta)$. Davison (2001) developed a hybrid LES/ RANS method through combining a one-equation sub-grid-scale model with a k-ω model for prediction recirculating flows. Camelli and Löhner (2002) blended B-L (Baldwin and Lomax, 1978) and Smagorinsky (1963) model through hybrid of the profile of eddy viscosity to calculate the separated flows. Inagaki et al. (2002) used a mixed-time-scale sub-grid scale model with fixed model parameters for practical LES. Hassan et al. (2003) developed a kind of zonal LES/RANS hybrid method for supersonic cavity flows, which refers to use of flow dependent blending functions to shift the closure from RANS in near-wall region to LES in outer part of boundary layer and in regions of local separation. Recently, M. Germano (2004) defined a hybrid additive filter that transitions smoothly from LES to RANS and discussed the property of the filter. Of course, there must be some other kinds of hybrid methods which are not listed here. In all the hybrid methods, the DES method (Squires et al. 2001; Forsythe et al., 2002; Viswanathan et al., 2003; Kotapati et al., 2004; Kotapati et al., 2004; Constantinescu and Squires,

2004; et al.) is the most widely used.

In the present study, the following hybrid approaches are adopted: one combines the LES-type Smagorinsky model with algebraic B-L model, DES based on S-A model, and DES and zonal hybrid methods based on Menter's k-ω SST model. The turbulence models are applied near the wall while the LES-type sub-grid model is employed for the regions of separation and away from the wall.

When solving the N-S equations with LES/RANS hybrid methods, several numerical schemes, such as the 4th-order Jameson-type central scheme with particle artificial viscosity, and second order LU-SGS-τTS method are applied in this study. Details of the LES/RANS hybrid methods and their switching criterion, as well as the numerical algorithms are discussed in the following paper.

LES/RANS HYBRID METHODS

The motivation of LES/RANS hybrid model was to combine LES with the best feature of RANS models. RANS models have been demonstrated an ability to predict attached flows very well with a relatively low computational costs. LES showed an ability to compute the separated flows accurately but at high cost for configuration with boundary layers.

The turbulence closure model is a term arising from the Reynolds averaged N-S equations. The Reynolds-stress tensor term is defined as

$$\tau_{ij} = -\overline{u_i' u_j'} \tag{1}$$

with u_i' denoting to the fluctuating velocity u-component and the over-bar represents the time average. The Reynolds-stress tensor is modeled in the Smagorinsky sub-grid closure as

$$\tau_{ij} = 2\nu_{Sma} S_{ij} \quad , \qquad \nu_{Sma} = C_S \Delta^2 \left(S_{ij} S_{ij}\right)^{1/2} \tag{2}$$

The local strain rate, S_{ij}, is defined as $S_{ij} = 0.5\left(\partial u_i/\partial x_j + \partial u_j/\partial x_i\right)$. C_S is the model constant, which lies in the range $0.01 < C_S < 0.05$. In this paper, C_S is not takes as a constant but a variable with the normal distance from the wall (Bui, 1999), which is given as:

$$C_S = 0.01\left(1.0 - \exp\left(-\left(\eta^+/25\right)^3\right)\right) \tag{3}$$

Hybrid method on Smagorinsky and B-L models

The present hybrid approaches consist of a blend of B-L and the Smagorinsky models, the algorithm to calculate the eddy/sub-grid viscosity for this hybrid method is depicted in Fig.1. The solid line represents the sub-grid viscosity of Smagorinsky model and the dashed line is that of B-L model. The parameter y_{eq} is the distance where the eddy viscosity of B-L model equals to that of the Smagorinsky sub-grid viscosity. When y is less than y_{eq}, the viscosity of the hybrid method takes that of B-L model; otherwise, the Smagorinsky sub-grid viscosity is employed.

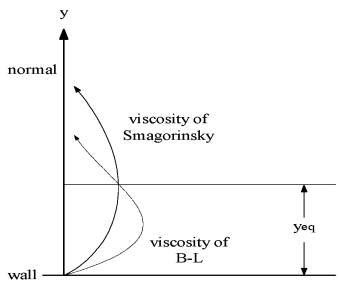

Fig.1 The viscosity of hybrid method based on B-L and Smagorinsky models

DES on S-A and Menter's k-ω SST models

Spalart's DES method is a hybrid of LES and RANS, which combines the strengths of both LES and RANS. Here, although we have no plan to list the original turbulence model equations, the formation of DES needs to be presented.

It is well known that the S-A model requires a partial differential equation (4) to be solved for a working variable $\hat{\nu}$ which is related to the turbulent viscosity. The differential equation is derived by "using empiricism and arguments dimensional analysis, Galilean invariance and selected dependence on the molecular viscosity" (Spalart, 1992). It should be mentioned here that the modification of natural laminar-turbulent transition (Deck, 2002) was introduced to calculate the transition when the flow is uncertain tripped. The model includes eddy viscosity production, near-wall turbulence destruction, diffusion and transition damping of production and transition of turbulence of source.

$$D\hat{\nu}/Dt = C_{b1}(1-f_{t2})\tilde{S}\hat{\nu} - \left(C_{w1}f_w - C_{b1}/\kappa^2 f_{t2}\right)\left(\hat{\nu}/d\right)^2 + \left(\nabla\cdot\left((\nu+\hat{\nu})\nabla\hat{\nu}\right) + C_{b2}(\nabla\hat{\nu})^2\right)/\sigma + f_{t1}\Delta U^2 \tag{4}$$

The near-wall destruction term in this model is proportional to $\left(\hat{\nu}/d\right)^2$, where d is the distance to the closest wall. When this term is balanced with the production term, the eddy viscosity becomes proportional to $S_{ij}d^2$. The LES-type sub-grid eddy viscosity of Smagorinsky varies with the local strain rate, and the grid spacing: $\nu_{Sma} \propto \Delta^2 S_{ij}$. If d in S-A model is replaced with Δ, the length scale of the sub-grid, in the wall destruction term, the S-A model will act as a Smagorinsky LES model. To exhibit both RANS and LES behavior, d in S-A model is replaced by $\tilde{d} = \min\left(d, C_{DES}\Delta\right)$. When $d < C_{DES}\Delta$, the hybrid method acts in an S-A mode and when $d > C_{DES}\Delta$ the method acts in a Smagorinsky LES mode. Therefore the method switches into LES mode when the grid is locally refined. Here the grid spacing Δ is taken as the longest distance between the cell center and all the neighboring cell centers. The constant C_{DES} is takes as 0.65.

The Menter's k-ω SST model (Menter, 1994) combines several desirable elements of existing two-equation models. The two major features of this model are a zonal weighting of model coefficients and a limitation on the growth of the eddy viscosity in rapidly strained flows. The zonal modeling uses Wilcox's k-ω model, which are well behaved near solid walls where low-Reynolds number corrections are not required and the standard k-ε model (in a k-ω formulation), which are relatively insensitive to free-stream values, near boundary layer edges and in free-shear layers. This switching is achieved with a flow dependent blending function. The SST modeling also modifies the eddy viscosity by forcing the turbulent shear stress to be bounded by constant times the turbulent kinetic energy inside boundary layers. This modification improves the prediction of flows with strong adverse pressure gradients and separation.

To construct DES-type hybrid methods based on two-equation models, some transformation is adopted in the turbulence kinetic equation. Then the final turbulence kinetic equation after introducing length scale is given as

$$\partial(\rho k)/\partial t + \partial\left(\rho u_j k - (\mu + \sigma_k)\partial k/\partial x_j\right)/\partial x_j = P_k - \rho k^{3/2}/l \tag{5}$$

where the length l is defined as $l = k^{1/2}/\left(\beta^* \omega\right)$. The ω-equation is just the same as that of original model.

The DES modification replaces the length scale l by $\tilde{l} = \min\left(l, C_{DES}\Delta\right)$ in equ.(5), where Δ is the length scale of the sub-grid and $C_{DES} = (1-F_1)C_{DES}^{k-\varepsilon} + F_1 C_{DES}^{k-\omega}$, where F_1 is the blending function; the constants $C_{DES}^{k-\varepsilon} = 0.61$, $C_{DES}^{k-\omega} = 0.78$. When $l < C_{DES}\Delta$, the hybrid method acts in the SST model; When $l > C_{DES}\Delta$, the method acts in a Smagorinsky LES mode. When the turbulence production is balanced with the destruction, $\tilde{l} = C_{DES}\Delta$, $k = \beta^*\left(C_{DES}\Delta\right)^2 S$, and $P_k = \rho\nu_t S = D_k = \rho k^{3/2}/\tilde{l}$, where $S = \left(\partial u_i/\partial x_j + \partial u_j/\partial x_i\right)\partial u_i/\partial x_j$. The final eddy viscosity is given as

$$\nu_t = \left(\beta^*\right)^{1.5}\left(C_{DES}\Delta\right)^2 S^{1/2} \propto S^{1/2}\Delta^2 \tag{6}$$

From Equ.(6), the eddy viscosity is similar with that of Smagorinsky model. When the grid is locally refined, the hybrid method will act as in a LES mode.

Zonal LES/RANS method

The zonal hybrid of LES/RANS method was originally developed from the idea of Menter's *k-ω* SST model. This method utilizes a blending function Γ, which is dependent on the distance from the nearest solid wall, to switch the closure from Menter's *k-ω* SST model near the wall to a one-equation sub-gird model away from the wall.

The particular form chosen for the turbulence kinetic energy equation is as follows:

$$\partial(\rho k)/\partial t+\partial\left(\rho u_j k-(\mu+\sigma_k)\partial k/\partial x_j\right)/\partial x_j=P_k-\rho\left(\Gamma\beta^* k\omega+(1-\Gamma)C_d k^{3/2}/\Delta\right) \quad (7)$$

and the eddy viscosity is given by

$$\mu_t=\Gamma(\rho k/\omega)+(1-\Gamma)\left(\rho C_s k^{1/2}\Delta\right) \quad (8)$$

where C_d and C_s is the constant, and Δ is a filter width defined as the cubic of the local cells volume. In the limit of balancing subgrid production and dissipation, the preceding model returns a Smagorinsky-type subgrid eddy viscosity: $\nu_t=C_s(C_s/C_d)\Delta^2\Omega$. In this study, both C_d and C_s are equal to 0.01.

So many kinds of blending function can be chosen from XIAO et al (2004). Such functions have the following common feature: Γ is equal to one near the solid wall while Γ becomes zero far way from the wall.

In this paper the blending function is chosen as

$$\Gamma=\tanh(\zeta^4),\ \zeta=\max(\tau_1,\ \tau_2),\ \tau_1=500\nu/(d^2\omega),\ \tau_2=k^{1/2}/(0.09d\omega) \quad (9)$$

The turbulence frequency ω is obtained from its transport equation as presented in its original form, which is formulated so that its production term does not depend on the eddy viscosity. Thus, the ω equation is only weakly influenced by the changing eddy viscosity and turbulence kinetic energy as the model shifts from RANS to LES mode. When the blending function is unity in Equs.(7) and (8), the RANS component dominates, whereas the LES component dominates when the blending function is zero. All constants appearing in the modified blending function and in Menter's model are the same as the original form.

NUMERICAL SCHEMES

The computations in this article are all based on a 3-D compressible solver with a modified Jameson-type cell-centered finite-volume formulation and a modified LU-SGS method with pseudo time sub-iteration implicit time stepping. Artificial dissipation with fourth order difference is used for unphysical oscillation suppression. Implicit residual smoothing was employed to accelerate the convergence. Uniform time stepping is applied to capture the unsteady properties in the flow.

Jameson-type Central Scheme

To enhance the robustness of artificial dissipation, the original scheme (Jameson, 1981) is modified here. They are:

1) Anisotropic artificial dissipation (Swanson, 1987) is applied to reduce the effect of artificial dissipation to the physical viscosity;
2) 4-order (Usta, 2002) central scheme is obtained though

$$\overline{F}_{i+1/2}=\left(-\overline{F}_{i-1}+7\overline{F}_i+7\overline{F}_{i+1}-\overline{F}_{i+2}\right)/12 \quad 0)$$

where $\overline{F}_i$ is the advective flux in i direction.

At far field boundaries, the 1-D Rieman characteristic analysis is employed to construct a non-reflection boundary condition (BC). For smooth surfaces, no-slip BC is used. Periodical BC for Aerospatial A-profile and symmetric BC for the prolate spheroid are applied.

LU-SGS-*τ*TS time stepping

The original LU-SGS scheme, which was developed by Yoon and Jameson (1987), is unconditionally stable and completely vectorizable. However, the explicit treatment of the viscous terms, the approximation of the flux Jacobian matrices and the linearization procedure in this scheme reduce the temporal accuracy. To achieve a higher accuracy in time, a Newton-like sub-iteration is introduced with a pseudo time (Jie et al., 2003), using the same approximation in the original method, the time-stepping method in this paper can be written as

$$(L+D)D^{-1}(D+U)\Delta\overline{Q}^m=-\left(3\overline{Q}^m_{i,j,k}-4\overline{Q}^n_{i,j,k}+\overline{Q}^{n-1}_{i,j,k}\right)/2-\Delta t\overline{R}^m_{i,j,k} \quad (11)$$

$$L=-\alpha(A^+_{i-1,j,k}+B^+_{i,j-1,k}+C^+_{i,j,k-1}),\ U=\alpha(A^-_{i+1,j,k}+B^-_{i,j+1,k}+C^-_{i,j,k+1}),$$

$$D=1.5\times I+\alpha\chi(\sigma_A+\sigma_B+\sigma_C)I+2\alpha\nu I$$

The initial values for the sub-iteration are taken as $\overline{Q}^0_{i,j,k}=\overline{Q}^n_{i,j,k}$. Starting with *m*=0, the sequence of iteration $\overline{Q}^m_{i,j,k}$, m=1, 2, 3 … converges to $\overline{Q}^{n+1}_{i,j,k}$ until the right-hand unsteady residual is approach to zero.

When $\Delta\overline{Q}^m_{i,j,k}\to 0$, it means that the residual is converged in the pseudo time. The accuracy of the solution at each physical time step is the accuracy of the discrete unsteady governing equations. That is to say, in the case of convergence, $\overline{Q}^{m+1}_{i,j,k}\to\overline{Q}^{n+1}_{i,j,k}$, and $\overline{R}^{m+1}_{i,j,k}\to\overline{R}^{n+1}_{i,j,k}$, then the following equation is valid,

$$\left(3\overline{Q}^{n+1}_{i,j,k}-4\overline{Q}^n_{i,j,k}+\overline{Q}^{n-1}_{i,j,k}\right)/2+\Delta t\overline{R}^{n+1}_{i,j,k}\to 0 \quad (12)$$

while the residual $\overline{R}^{n+1}_{i,j,k}=(\delta\overline{F}^{n+1}_{i,j,k}-\delta\overline{F}^{V\ n+1}_{i,j,k}/\mathrm{Re})/Vol_{i,j,k}$, then Equ.(12) yields a second-order fully implicit scheme in time,

$$Vol_{i,j,k}\frac{3\overline{Q}^{n+1}_{i,j,k}-4\overline{Q}^n_{i,j,k}+\overline{Q}^{n-1}_{i,j,k}}{2\Delta t}+\delta\overline{F}^{n+1}_{i,j,k}=\frac{1}{\mathrm{Re}}\delta\overline{F}^{V\ n+1}_{i,j,k} \quad (13)$$

The computing practices show that the rate of convergence with the pseudo time level is very fast, and only a few sub-iterations are needed.

RESULTS AND DISCUSSION

It must be mentioned that the chord length of Aerospatial A-profile (*C*) and the long-axis of prolate spheroid (*2a*) are chosen as the characteristic length (*L*) respectively.

The grids around the Aerospatial A-profile and prolate spheroid are shown in Fig. 2. 360×16×86 grids are around A-profile in the streamwise, spanwise and normal direction, and 121×101×86 grids are around prolate spheroid in the streamwise, circular and normal direction. The minimum grid spacing near the solid surface is 7.5×10^{-6} and the spanwsie width is 5% for Aerospatial A-profile. For the prolate spheroid, the grids of leeside and aft-body are clustering for capturing the structure of vortices.

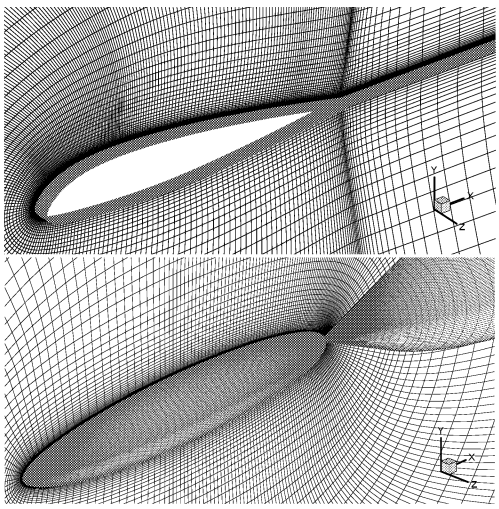

Fig. 2 3-D grids around the Aerospatial A-profile and prolate spheroid

The length scale associated with the smallest turbulent

motions for these flows can be evaluated from an estimate of Kolmogorov length scale given by $\lambda_K=\beta^{-1/4}Re_l^{-3/4}$, whereas the length scale for the integral scale motions can be obtained from an estimate of the Taylor length scale given by $\lambda_T=15^{1/2}(\beta Re_l)^{-1/2}$, where β is a constant of $O(1)$, l the bulk integral scale (the characteristic length L) and Re_l the integral scale Re number (while the freestream Reynolds number $Re_L=v_0L/v$). For $Re_L=2.1\times10^6$ (Aerospatial A-profile) or 6.5×10^6 (prolate spheroid) these length scales are $\lambda_K = 2.15\times10^{-5}$ or 9.225×10^{-6} L and $\lambda_T=3.76\times10^{-3}$ or $2.14\times10^{-3}L$, respectively. The smallest grid spacing is in the vicinity of the hull to resolve the velocity gradients and the wall shear stress. In the present mesh, the characteristic cell sizes $\Delta=\sqrt[3]{Vol_{cell}}$ range from 1.28×10^{-5} or 2.86×10^{-5} L (close to the body) to 0.0193 or 0.0957 L (in the freestream). This implies that the large-scale eddies are reasonably well resolved and that the grids are appropriate for LES/RANS hybrid methods.

Aerospatial A-profile

The flow around a single airfoil at maximum lift is considered as one of the most difficult computational test case for RANS and LES methods, due to the extreme sensitivity of boundary layer separation to geometric and turbulence parameters. The free-stream Mach number is 0.15, AOA is 13.3 deg. For the Aerospatial A-profile, initial conditions for hybrid simulations were obtained by solving the flowfields in two-dimensions using RANS methods based on only B-L and S-A models.

The numerical results compared with the experiment, which include surface pressure and skin friction coefficients and the profile of velocity at three upper sections (x/C=50, 70 and 90%), are shown in Fig. 3. All the results of hybrid methods are obtained through temporal and spatial average in span-wise direction. All the numerical results agree the experimental C_p well; whereas the values of DES on S-A model is just a little lower than the experiment. From the comparison of C_f, DES and RANS methods based on S-A model show the sudden decrease of C_f near the leading edge, which indicates the modification of S-A model can capture the flow transition automatically; although the numerical results are little lower than the experiment near the leading edge. From it we can learn that the hybrid of LES/RANS methods preserve the characteristics of the fundamental turbulence model near the wall. The results of hybrid and RANS methods based on B-L model, which has not include the effect of history, show little difference and they match the experiment poor for profile of velocity. However, S-A model exhibits the ability of simulating the flow separation and recirculation near the trailing edge. The results of RANS method on S-A model match the experiment very well for the profile of velocity; while the DES method on S-A model shows little larger vortex near the trailing edge through the comparison of profile of velocity. The history of lift, which demonstrated strongly unsteadiness feature, using DES methods based on S-A model is also shown. Some instantaneous and temporal-averaged vortices near the trailing edge using iso-surface (u=0.05(blue), 0.625(green) and 1.0(red)) of velocity u are demonstrated in Fig.4. The large-scale of vortices generated and detached from the shear flows ceaselessly.

Prolate spheroid

The simplicity of the body geometry should not give rise to the assumption that the flow features are as simple as the body configuration. In contrast, the flow field is rather complex, exhibiting pressure induced-vortex sheet-separation. At high AOA, several separation and reattachment lines do appear on the leeward side surface. In the present study, the case is not based on the experiment of Wetzel (1998) but Kreplin (1995). The free stream Mach number is 0.25, and the AOA is 30 deg. The flow with natural transition exhibits two mainly phenomena: (1) On the pressure side, a large laminar area appears; (2) On the leeward side, the separation is very complex with cross flow reversals indicating multiple separation and reattachment.

The initial conditions for hybrid simulations started from the fields solving with RANS turbulence model of B-L, S-A and Menter's k-ω SST models. For the prolate spheroid, the hybrid methods based on B-L, S-A and Menter's k-ω SST models are all used to simulate the complex separated flow. However, we are mainly focus on studying the effect of hybrid and RANS methods on SST model.

The surface pressure and skin friction coefficients at three different sections ($x/2a$=48, 56 and 73%) using hybrid methods and RANS on SST model are compared with the experimental data. A very good agreement of calculation of C_p with measurements can be seen in Fig. 5. It's very difficult to simulate the pressure increase towards the rear of the body on the leeward side. The hybrid based on B-L model underpredicts the pressure minimum on the leeward side, which is little overpredicted using the hybrid method on S-A model. Although RANS on k-ω SST model underpredicts the pressure minimum a little, it shows different pattern comparing with that of hybrid on B-L model. The DES and zonal hybrid methods on k-ω SST model agree with the measurements reasonably well. In the laminar region, the computational results show a much higher plateau of shear (Cf) while the measurements are much lower. However, from the physics transition region up to the crown line, the numerical results show good recovery of the flow. The DES on S-A model shows better agreement with the experiment in the laminar region. In the separated region on the leeward side, RANS on k-ω SST model shows poor with other methods and the measurement. The comparison of circumferential wall shear stress angle distribution (γ) show that the results using hybrid on B-L model overestimate the azimuthal extent of separation region, while the other results agree the measurements very well.

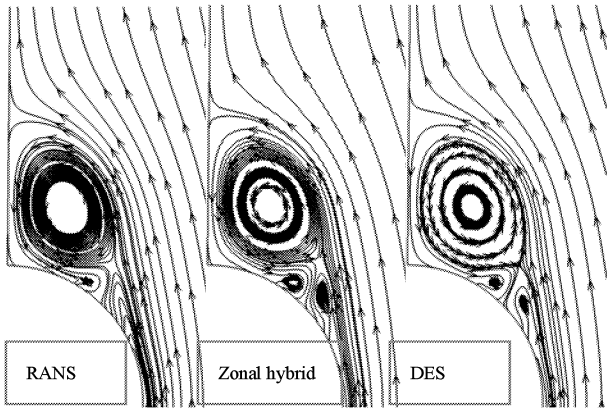

Fig. 7 Cross flow streamline pattern at x/2a=73% based on k-ω SST model

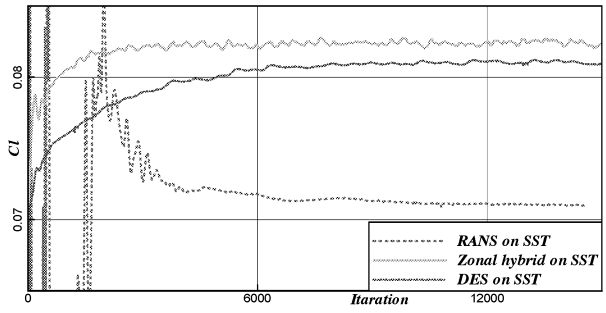

Fig.8 Lift history based on SST model

Primary, secondary, even tertiary separation and reattachment regions using hybrid and RANS methods based on k-ω SST model are demonstrated in Fig. 6. The distinct difference is the distribution of the surface tracelines on the leeward side, the shape and strength of the primary vortex. At the same time, Fig. 7 displays the cross flow pattern at section x/2a=0.73.

The history of lift is demonstrated in Fig. 8. From it we know that the flow using RANS method is converged after step 6000, however, the lift using hybrid methods shows some little fluctuations.

CONCLUSION

High Reynolds flowfields predictions around Aerospatial A-profile and prolate spheroid at high angle of attack were obtained using both hybrid of LES/RANS and RANS methods based on B-L, S-A and Menter's k-ω SST models. Unsteady, large-scale motions are calculated successfully using hybrid methods based on traditional turbulence models. According to the comparison between the calculations and experimental measurements, the results using LES/RANS hybrid methods almost show more reasonable than RANS methods based on the same turbulence models.

However, generally spoken, the behavior of LES/RANS hybrid methods mainly depends on the fundamental turbulence models. So, if we design the LES/RANS hybrid method based on turbulence models with powerful capability for simulating separation, this kind of hybrid method is possibly suitable for the separated flows. The hybrid and RANS methods based on S-A and Menter's k-ω SST models show much reasonable agreement with measurements for adverse pressure gradient flows than that based on the algebraic B-L model, which is in defect of history.

ACKNOWLEDGMENT

This project was supported by China Postdoctoral Science Foundation and National Natural and Science Foundation of China under Contract 10477012 and 10232020, and the China NKBRSF project 2001CB409600.

.

REFERNCE

C.P. Mellen et al., "Lessons from LESFOIL Project on Large-Eddy Simulation of Flow around an Airfoil," *AIAA Journal*, vol.41, No.4, April, 2003, pp. 573-581.

S. Dahlström and L. Davidson, "Large Eddy Simulation of the Flow around an Aerospatiale A-Aerofoil," *European Congress on Computational Methods in Applied Science and Engineering,* Sep., 2000.

P.E. Morgan and M.R. Visbal, "Large-Eddy Simulation of Airfoil Flows," *AIAA* 2003-0777, Jan., 2003.

C.-Y. Tsai and A.K. Whitney, "Numerical Study of Three- Dimensional Flow Separation for a 6:1 Ellipsoid," *AIAA* 99-0172, Jan., 1999.

Spalart P.R., and Allmarars S.R., "A One-Equation Turbulence Model for Aerodynamic Flows," *AIAA* 92-0439, Jan., 1992.

G.S. Constantinescu et al., "Numerical Ivestigation of Flow Past a Prolate Spheroid," *AIAA* 2002-0588, Jan., 2002.

N. Wikström et al., "Large Eddy Simulation of the Flow around an Inclined Prolate Spheroid," Journal of Turbulence, No.5, 2004.

Spalart, P.R. et al., "Comments on the Feasibility of LES for Wing and on a Hybrid RANS/LES Approch", *Advance in DNS/LES, 1st AFOSR Int. Conf. on DNS/LES*, Aug.4-8, 1997, Greyden Press, Columbus OH.

Speziale, C. G., "Turbulence Modeling for Time-Dependent RANS and VLES: A Review," *AIAA Journal*, Vol. 36, No. 2, 1998, pp. 173–184.

Strelets, M., "Detached Eddy Simulation of Massively Separated Flows," *AIAA* 2001-0879, Jan. 2001.

Menter, F. R., "Two Equation Eddy Viscosity Turbulence Models for Engineering Applications," *AIAA Journal*, Vol. 32, No. 8, August, 1994, pp. 1598–1605.

L. Davidson, "Hybrid LES-RANS: a Comparison of a One-Equation SGS model and a k-ω model for Prediction Recirculation Flows," *European Congress on Computational Methods in Applied Science and Engineering, Compustational Dynamics Conference 2001*, Sep. 2001.

F.E. Camelli and R. Löhner, "Combining the Baldwin-Lomax and Smagorinsky Turbulence Models to Calculate Flows with Separation Regions," *AIAA* 2002-0426, Jan., 2002.

Bladwin B., and Lomax H., "Thin-Layer Approximation and Algebraic Model for Separation Flows," *AIAA* 78-257, Jan. 1978.

Smagorinsky J., "General Circulation Experiments with Primitive Equations. I. The Basic Experiment," *Mon. Weather Rev.*, 1963, 91: 99-164.

M. Inagaki et al., "a mixed-time-scale sub- grid scale model with fixed model parameters for practical LES", *Engineering Turbulence Modeling and Experiments-5*, Elsevier Science Ltd., 2002, pp: 257-266.

R.A. Baurle et al., "Hybrid Simulation Approach for Cavity Flows: Blending, Algorithm, and Boundary Treatment Issues," *AIAA Journal*, Vol. 41, No. 8, Aug. 2003, pp: 1463-1480.

M. Germano, "Properties of the hybrid RANS/RANS filter," *Theoretical Compu. Fluid Dynamics*, Vol. 17, 2004, pp: 225-231.

K.D. Squires, et al, "Progress on Detached-Eddy Simulation of Massively Separated Flows," *AIAA* 2002–1021, Jan., 2002.

J.R. Forsythe et al., "Detached-Eddy Simulation With Compressibility Corrections Applied to a Supersonic Axisymmetric Base Flow," *Journal of Fluids Engineering*, Vol.124, Dec., 2002, pp: 911-923.

A.K. Viswanathan et al., "Detached-Eddy Simulation around a Forebody at High Angle of Attack," *AIAA* 2003–0263, Reno, Jan., 2003.

R.B. Kotapati et al., "Prediction of the Flow over an Airfoil at Maximum Lift," *AIAA* 2004-0259, Jan., 2004.

V. Krishnan et al., "Prediction of Separated Flow Characteristics over a Hump using RANS and DES," *AIAA* 2004-2224, July, 2004.

G. Constantinescu and K. Squires, "Numerical investigations of flow over a sphere in the subcritical and supercritical regimes", *PHYSICS OF FLUIDS*, Vol. 16, No.5, May, 2004, pp: 1449-1466

T.T. Bui, "A parallel, Finite-Volume Algorithm for Large-Eddy Simulation of Turbulent flows," *NASA/TM*-1999-206570, Jan., 1999

S. Deck et al., "Development and Application of Spalart-Allmaras one-Equation turbulence model to three-dimensional supersonic complex configurations," *Aerospace Science and Technology*, No.6, 2002, pp: 171-183.

X. Xiao et al., "Blending Functions in Hybrid Large-Eddy/Reynolds -Averaged Navier-Stokes Simulations," *AIAA Journal*, Vol. 42, No. 12, Dec., 2004, pp: 2508-2515.

Jameson A. et al., "Numerical Solutions of Euler Equations by Finite Volume Methods with Runge-Kutta Time Stepping Schemes", *AIAA Paper* 81-1259, 1981.

Swanson R.C. and Turkel E., "Artificial Dissipation and Central Difference Schemes for Euler and N-S Equations," *AIAA* 87-1107, 1987.

E. Usta, "Application of a Symmetric Total Variation Diminishing Scheme to Aerodynamic of Rotors," *Doctor Thesis*, Georgia Institute of Technology, August 2002.

Yoon S. and Jameson A., "Lower-Upper Symmetric-Gauss-Seidel Method for the Euler and Navier-Stokes Equations," AIAA 87-0600, 1987

Li Jie et al., "A fully implicit method for steady and unsteady viscous flow simulations", *Journal for Num. Methods in Fluids*, vol. 43, 2003, pp: 147-163

T.G. Wetzel et al., "Measurement of Three-Dimensional Crossflow Separation," *AIAA Journal*, Vol. 36, No. 4, April 1998, pp: 557-564

Kreplin, H.P, "Three-dimensional boundary layer and flow field data of an inclined prolate spheroid," *AGARD FDP WG-14 Experimental test cases for CFD validation, Test Case ID: GE-20,* 1995.

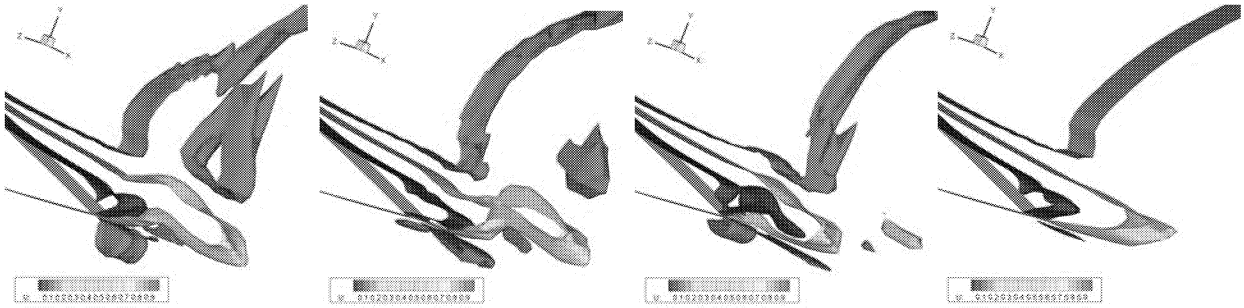

Fig. 4 The instantaneous and temporal-averaged iso-surface of velocity of u with DES on S-A model

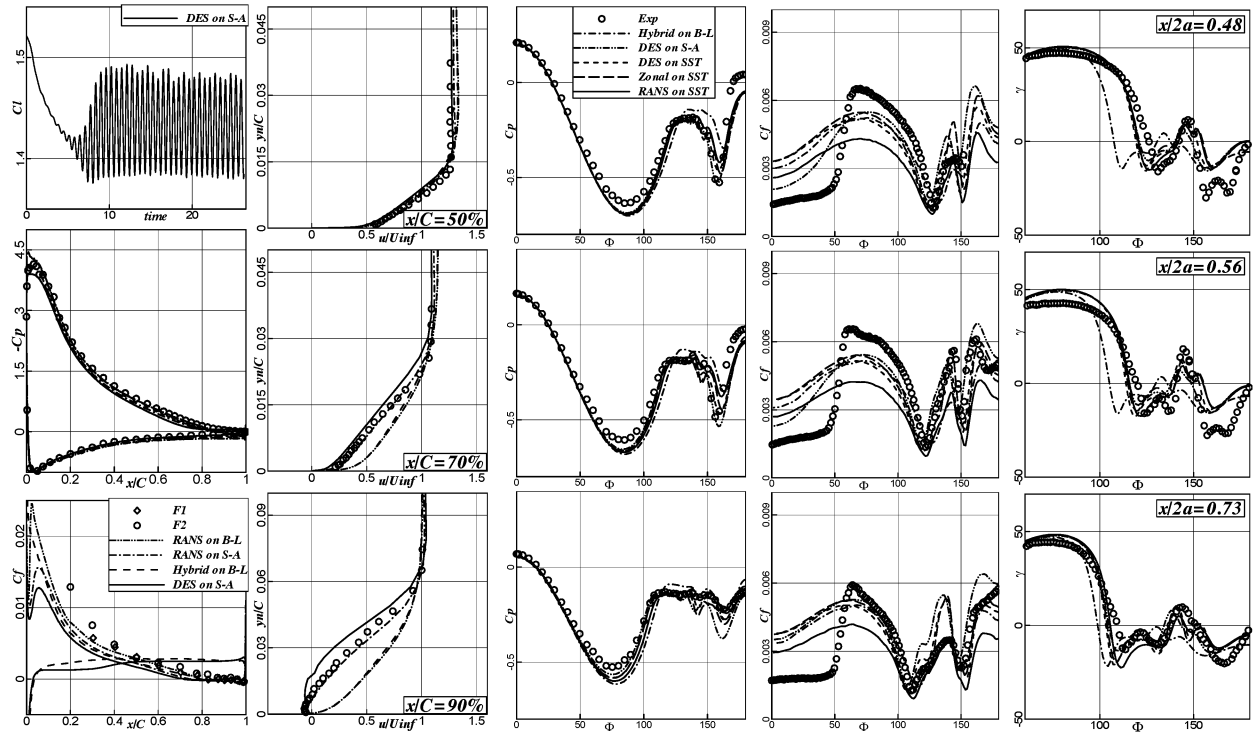

Fig.3 Results using hybrid and RANS on B-L and S-A models

Fig. 5 Results using hybrid and RANS for C_p, C_f and γ

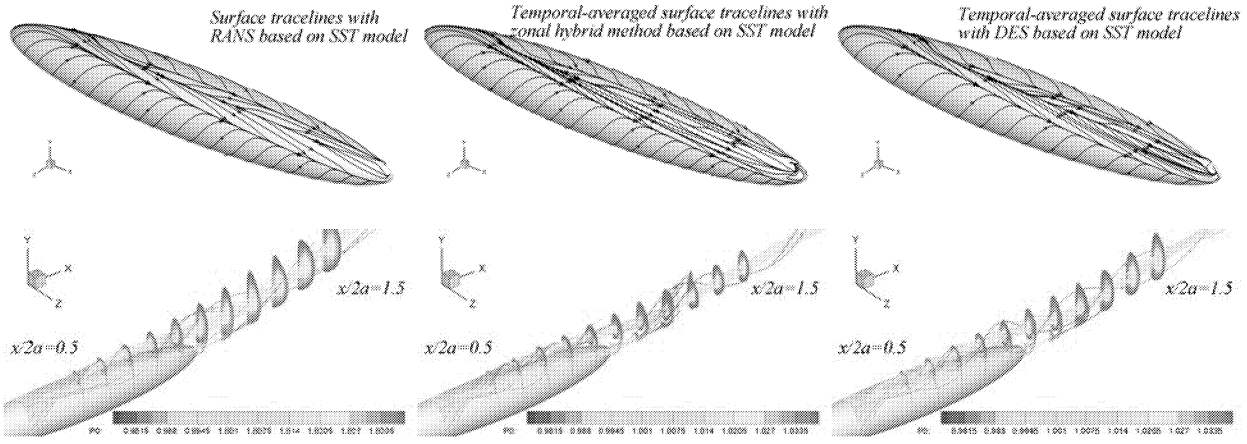

Fig.6 Temporal-averaged surface trace-lines and vortices based on Menter's k-ω SST model